

HD 112 μm in absorption and extreme CO depletion in a cold molecular cloud^{*}

E. Caux¹, C. Ceccarelli^{2,3}, L. Pagani⁴, S. Maret¹, A. Castets², and J. R. Pardo⁵

¹ CESR CNRS-UPS, BP 4346, 31028 Toulouse Cedex 04, France

² Observatoire de Bordeaux, BP 89, 33270 Floirac, France

³ Laboratoire d'Astrophysique, Observatoire de Grenoble, BP 53, 38041 Grenoble Cedex 09, France

⁴ LRM-DEMIRM, 77 avenue Denfert Rochereau, 75014 Paris, France

⁵ Consejo Superior de Investigaciones Científicas (CSIC), Madrid

Received 13 November 2001 / Accepted 21 December 2001

Abstract. We present ISO-LWS observations at high spectral resolution ($R \sim 10^4$) towards a cold molecular cloud in the line of sight of W49. The HD ground state transition at 112 μm is detected, showing the first observation of this line in absorption outside the solar system. The 112 μm absorption depth gives a straightforward measure of the lower limit of the cloud's HD column density, $N(\text{HD}) > 8 \times 10^{18} \text{ cm}^{-2}$. We also mapped the same line of sight in the ^{12}CO (2–1) and (3–2), and ^{13}CO (2–1) transitions at the CSO, and in the C^{18}O and C^{17}O (1–0) and (2–1) transitions at the IRAM 30-m. From these observations we derive an upper limit to the CO column density, $N(\text{CO}) < 7 \times 10^{17} \text{ cm}^{-2}$. Assuming a standard CO abundance (1×10^{-4}) would imply a $[\text{D}]/[\text{H}]$ abundance two orders of magnitude larger than the average $[\text{D}]/[\text{H}]$ value observed in the solar neighborhood. The alternative explanation that we defend here is that CO is highly depleted (by a factor 100) in this cloud. This is the first measurement of such a depletion factor in a relatively massive cold molecular cloud ($\sim 10^3 M_{\odot}$).

Key words. ISM: abundances – ISM: lines and bands – ISM: molecules – ISM: clouds – ISM: individual objects: W49 – infrared: ISM – radio lines: ISM

1. Introduction

As widely known, deuterium is thought to be produced in the early Universe and its abundance is thought to be a sensitive measure of the baryonic mass of the Universe. An observational effort has been made, aimed at measuring the $[\text{D}]/[\text{H}]$ ratio in a variety of astrophysical conditions (for a recent review see e.g. Vidal-Madjar et al. 1998). Despite the many efforts, the D abundance remains poorly known except in the immediate vicinity of the solar system ($\sim 2 \times 10^{-5}$), where it is probably known within an uncertainty of 20% (Linsky et al. 1995; Linsky & Wood 1996; Sonneborn et al. 2000). The two recent space missions, ISO (Kessler et al. 1996) and FUSE (Moos et al. 2000), have been expected to provide measures of the $[\text{D}]/[\text{H}]$ ratio farther out, by measuring the HD/ H_2 ratio in distant molecular clouds by means of the HD lines in the FIR and UV respectively (e.g. Ferlet et al. 2000). So far ISO has detected HD in emission towards Orion, at $\sim 450 \text{ pc}$

from the Sun (Wright et al. 1999; Bertoldi et al. 1999). The derived $[\text{D}]/[\text{H}]$ ratio is smaller than the value measured in the solar neighborhood ($0.8\text{--}1 \times 10^{-5}$), but some uncertainty in this estimate lies in the method used which relies on some modeling of the observed line fluxes. In principle a clean determination of the $[\text{D}]/[\text{H}]$ ratio can be obtained when the HD ground rotational transition at 112 μm is seen in absorption in molecular clouds, where both hydrogen and deuterium are in the molecular form. The 112 μm absorption depth would give a straightforward measure of the amount of HD in the line of sight, whereas several methods could give a reliable measure of the H_2 column density, although not straightforward if neither H_2 nor CO are seen in absorption in the same line of sight.

In this paper we report the first ever detection of the HD 112 μm line in absorption in a molecular cloud. This observation was performed along a line of sight aiming at the W49 star forming region center. The HD observations are accompanied by CO millimeter observations, to measure the H_2 column density along the same line of sight. Surprising enough, the comparison between the derived HD and CO column densities indicates the presence of a cloud in the line of sight, which is dramatically deprived of CO, as discussed in Sect. 4.

Send offprint requests to: E. Caux, e-mail: caux@cesr.fr

^{*} Based on observations with ISO, an ESA project with instruments funded by ESA Member States (especially the PI countries: France, Germany, The Netherlands and the UK) with the participation of ISAS and NASA.

2. Observations and results

The W49 region is one of the largest star forming regions in our Galaxy (Scoville & Solomon 1973). It is very bright in the FIR and lies at 11.4 kpc from the Sun behind the Galactic Center (Gwinn et al. 1992). The line of sight towards W49 crosses twice the Sagittarius arm, where several atomic and molecular clouds lie (Nyman 1983). All this makes the W49 direction a good target to study lines from these molecular clouds in absorption against its strong continuum.

We therefore used ISO-LWS to carry out observations of the HD ground state rotational transition ($\nu = 0 - 0$, $J = 1 \leftarrow 0R(0)$). The rest wavelength of this transition is $112.072506 \pm 0.000007 \mu\text{m}$ (Evenson et al. 1988). No observations were done with SWS on this line of sight, preventing a direct determination of the H_2 column density. In order to derive the H_2 column density and therefore the D/H ratio, we mapped the emission from the transitions below 350 GHz of CO isotopes, covering the ISO-LWS beam. The two following sub-sections describe the HD and CO observations separately.

2.1. ISO-LWS observations of HD

High spectral resolution observations of the HD ground state transition at $112 \mu\text{m}$ were performed using the Long Wavelength Spectrometer instrument (hereafter LWS: Clegg et al. 1996) on the ISO satellite (Kessler et al. 1996). These observations were obtained during revolution 316 in a Fabry-Pérot mode (LW04). They consisted of three independent sets of fourteen LWS-FP scans centered on the rest frequency of the HD line ($t_{\text{int}} = 16.8\text{s}$ for each sampled point). The ISO-LWS beam was centred on the coordinates: $\alpha_{2000} = 19^{\text{h}}10^{\text{m}}17^{\text{s}}.5$, $\delta_{2000} = 9^{\circ}05'59.5''$. The data were sampled at 1/4 of the FP resolution element and seven spectral elements on either side of the line were acquired. The *FWHM* beam of the detector used (LW2) is $\sim 78''$. The resolving power at this wavelength measured on the ground was 9650, or $\sim 31 \text{ km s}^{-1}$. The wavelength calibration accuracy of the LWS-FP is $\pm 11 \text{ km s}^{-1}$ (Gry et al. 2001). A full range 43–197 μm grating spectrum was also obtained for the same line of sight during revolution 316, allowing to calibrate the data (fringes and continuum level). This observation is made of three scans sampled at 1/4 of the grating resolution element with an integration time on each sampled point of 1.2 s.

The initial data processing was carried out using the ISO-LWS Off-Line Processing software (v10), up to the Auto Analysis Result stage. Further data reduction was performed using the LWS Interactive Analysis software (LIA v10). During this step, the continuum level of the FP data was re-calibrated against the grating observations. This is needed because a grating positioning problem in LW04 mode introduces a spurious slope on the spectrum and because the dark current measurement does not take into account the stray-light and the error due to FP order sorting that affect LW04 measurements. A final analysis

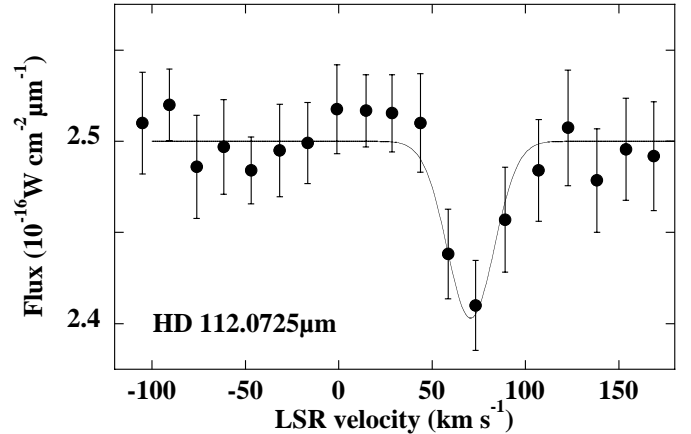


Fig. 1. ISO-LWS high resolution spectrum of the HD transition at $112 \mu\text{m}$ (black dots) and the fitted absorption line.

was made, using the ISAP package, to remove bad data points and to perform sigma-clipping and co-adding. ISO LW01 spectra are flux calibrated using Uranus, and the final absolute accuracy obtained is estimated to be better than 30% (Swinyard et al. 1998). The line is directly visible in 2 of the 3 data sets, and is clearly detected (Fig. 1) after co-adding of the 3×14 FP scans and smoothing to $5 \times 10^{-3} \mu\text{m}$ to improve the signal to noise ratio.

A clear absorption ($\sim 4\%$) of the strong continuum is observed around $V_{\text{LSR}} = (71 \pm 11) \text{ km s}^{-1}$, very far away from the V_{LSR} of W49 itself (8 km s^{-1}), but close to that of a molecular cloud on the line of sight ($V_{\text{LSR}} = 63.5 \text{ km s}^{-1}$, see Sect. 2.2). The line-width of this absorption is $(30 \pm 3) \text{ km s}^{-1}$, very similar to the measured spectral resolution of LWS at this wavelength (Gry et al. 2001). The line is therefore not resolved with the LWS spectrometer. The equivalent line width corresponding to this absorption is $W_{\lambda} = (4.3 \pm 1.7) \times 10^{-4} \mu\text{m}$. This value leads to a very high HD column density in this molecular cloud (relative to CO, see Sect. 3). We therefore checked very carefully the different steps of the data processing with the LIA and did not find any effect that would change the observed value of the absorption by more than 30%.

We are confident that the observed feature is real and is not the result of instrumental effects for the following reasons. First, even if the grating spectral responsivity calibration file (RSRF) has a spurious feature at $112 \mu\text{m}$, this is due to the presence of HD absorption in the spectrum of the calibration source (Uranus) which cannot affect our FP spectrum, whose width is $0.15 \mu\text{m}$, i.e. four times smaller than that of the grating spectral element at this wavelength. Second, spurious features can be expected on strong sources from leakage into the FP of adjacent spectral orders. The FP free spectral range at $112 \mu\text{m}$ is $1.12 \mu\text{m}$ and the only strong lines expected in the observed LWS range are the high- J transitions from ^{12}CO and ^{13}CO that could arise from W49 itself, but they would only be seen in emission. Third, we processed similar observations towards two other bright sources, Orion BN/KL and SgrB2 (Polehampton et al. 2002), both brighter than

W49 at $112\ \mu\text{m}$, with the result that both sources do not present any absorption at this wavelength.

2.2. CO observations

We first obtained ^{12}CO and ^{13}CO line maps at the CSO 10-m telescope (Caltech Submillimeter Observatory – Hawaii, USA) of the entire LWS beam. We then complemented these observations at higher spatial resolution observations around the brightest regions at the IRAM 30-m telescope (Pico Veleta, Spain). The two sets of observations are described separately in the following sections.

2.2.1. CSO 10-m observations

The CSO observations were performed in May 2001. We mapped the $78''$ ISO-LWS beam in the ^{12}CO (2–1) and ^{13}CO (2–1) lines (13 points spaced by $30''$) and in the ^{12}CO (3–2) line (44 points spaced by $20''$). We used two SIS receivers at 230 and 345 GHz, connected to two Acousto-Optical Spectrometers (AOS) that provide a spectral sampling of 48 kHz and 0.47 MHz respectively. Since we are only interested in the molecular clouds with velocities larger than $40\ \text{km s}^{-1}$, we centered the narrow (50 MHz) high resolution AOS on $V_{\text{LSR}} = 70\ \text{km s}^{-1}$ covering the range $40\text{--}100\ \text{km s}^{-1}$ at 230 GHz and $50\text{--}90\ \text{km s}^{-1}$ at 345 GHz. System temperatures during the observations were in the ranges 300–390 and 710–1190 K in the two bands respectively. The beam size is $34''$ at 230 GHz and $20''$ at 345 GHz. Pointing and focus were regularly monitored on Mars, and pointing corrections were always found smaller than $3''$. We corrected for the forward scattering and spill-over efficiency ($\eta_{\text{fss}} = 0.85$ for both frequencies) to set the results in the T_{R}^* scale. The obtained T_{R}^* ^{13}CO (2–1) map (Fig. 2), shows the presence of a cloud at $\sim 63.5\ \text{km s}^{-1}$ in the north part of the LWS beam. This

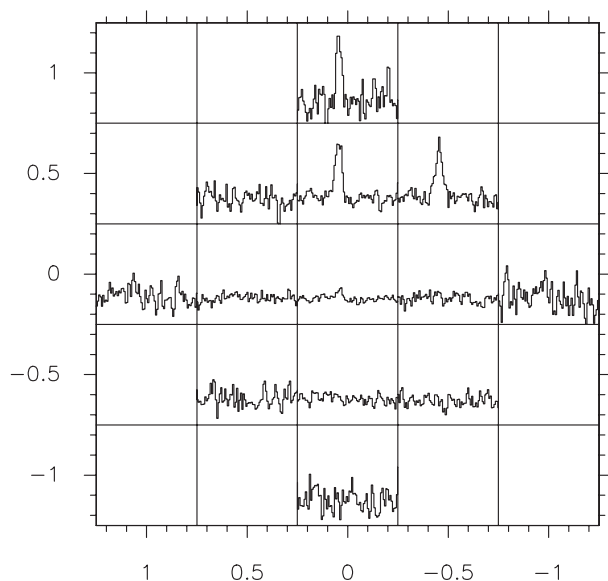


Fig. 2. ^{13}CO (2–1) line map. LSR velocity range is $[55, 75\ \text{km s}^{-1}]$, and temperature (T_{R}^*) range is $[-0.5, 1.4\ \text{K}]$. RA and Dec. offsets are in arcmin.

is certainly the component with the largest CO column density, as indicated by Fig. 3, which reports the profiles of the three observed lines, smoothed to the LWS beam.

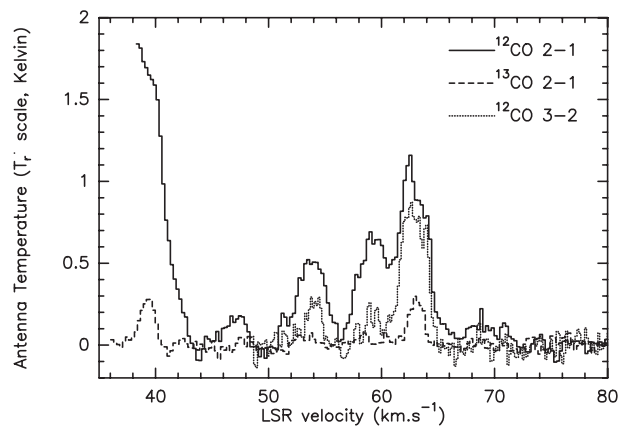


Fig. 3. ^{12}CO (2–1) and (3–2) and ^{13}CO (2–1) line spectra smoothed to the LWS beam. Velocity sampling is $0.25\ \text{km s}^{-1}$ for the 1.3 mm lines and $0.16\ \text{km s}^{-1}$ for the 0.8 mm line.

2.2.2. IRAM 30-m observations

We hence mapped this cloud with the higher angular resolution of the IRAM telescope in August 2001 (Director Discretionary Time). The observations consisted of maps in the C^{18}O and C^{17}O , (1–0) and (2–1) transitions. The scope was first to measure as best as possible the column density of the cloud, which is best probed by the (1–0) transition; second to check the clumpiness of the CO emission; third to have a reliable measure of the line opacity, looking for C^{17}O emission; finally, to have an estimate of the temperature of the cloud, we also observed the (2–1) transition for both isotopomers.

We used four SIS receivers simultaneously, at 109.8, 112.4, 219.6 and 224.7 GHz. The autocorrelator was split in 4 parts, with 40 kHz sampling at 2.7 mm and 80 kHz sampling at 1.3 mm. System temperatures were typically 150 K at 2.7 mm and 200–230 K at 1.3 mm. Pointing and focus were checked regularly on K3-50A. The beam size is $22''$ at 110 GHz and $11''$ at 220 GHz. The main beam efficiency is 0.8 at 110 GHz and 0.52 at 220 GHz. Though η_{fss} is not known, one can estimate it to be 0.87 at 110 GHz and 0.71 at 220 GHz. The resulting C^{18}O maps in the T_{R}^* scale are shown in Fig. 4. Comparison between the CSO and IRAM data shows that the IRAM spectrum is 90% brighter and 60% narrower. This is consistent with the AOS dilution of the signal together with the fact that the IRAM map does not extend far enough to cover entirely the CSO beam down to the 10%.

Finally, the C^{18}O 1–0 line is found 10 times stronger than the left-side component ($F: 5/2 \rightarrow 5/2$, 0.333 relative intensity) of the C^{17}O (1–0) line triplet, and the total area ratio is 3.9. The first relevant result of this mapping is hence that the C^{18}O (1–0) line is optically thin and we can use it to derive the CO column density in the cloud.

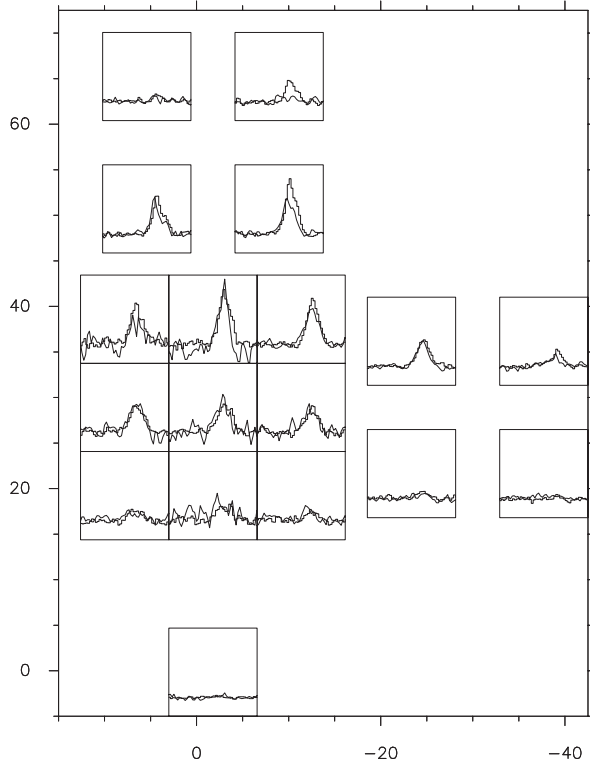


Fig. 4. $C^{18}O$ (1–0) (histogram) and (2–1) (normal) line spectra maps. Velocity range is $[60, 65 \text{ km s}^{-1}]$ and T_R^* range is $[-0.5, 1.8 \text{ K}]$. RA and Dec offsets are in arcsec.

Second, the cloud appears to be rather smooth on most of the IRAM beams (Fig. 4), ruling out the presence of a single very dense clump in the ISO beam.

3. Column densities

3.1. HD

The absorption depth of the $112 \mu\text{m}$ HD ground state transition gives a very clean measure of the HD column density along the line of sight. Assuming (very likely) that all the molecules are in the ground state and that the absorption is not thick, it yields (e.g. Spitzer 1978):

$$N(\text{HD}) = 3.12 \times 10^{22} W_\lambda \text{ cm}^{-2} \quad (1)$$

where W_λ is the line Equivalent Width (in μm) and using the Einstein coefficient for the spontaneous emission equal to $5.12 \times 10^{-8} \text{ s}^{-1}$ (Abgrall et al. 1982). Applying Eq. (1) gives a conservative *lower limit* to the HD column density, which may be larger if the absorption is thick (this can be the case as the line-width of the $C^{18}O$ line is only 0.8 km s^{-1} , to be compared with the ISO-LWS 30 km s^{-1} resolution) and/or if an important fraction of the HD molecules are not in the ground state. Since $W_\lambda = (4.3 \pm 1.7) \times 10^{-4} \mu\text{m}$, the *minimum HD column density* is $8 \times 10^{18} \text{ cm}^{-2}$.

3.2. CO and H_2

The most common H_2 tracers are the dust continuum and the CO emission. In our case, we cannot use the dust

continuum observations, as they lack the kinematic information and therefore cannot be attributed to the cloud at 63.5 km s^{-1} that absorbs the $112 \mu\text{m}$ photons. We therefore have to rely entirely on the CO observations to measure the H_2 column density of this cloud.

In order to compute the CO column density we need an estimate of the gas temperature. Actually, as the column density is derived from the $C^{18}O$ (1–0) observations, it is particularly sensitive to temperature values below $\sim 7 \text{ K}$. Changing the temperature from 7 K to 15 K would decrease the estimate of the CO column density by 25%. Using a LVG model, we found that solutions with temperatures below 7 K imply optically thick $C^{18}O$ lines and therefore are ruled out by the observations. Assuming a gas temperature of 7 K (in order to have the upper limit of the CO column density) gives an average $C^{18}O$ column density in the LWS beam of $5.5 \times 10^{14} \text{ cm}^{-2}$ for the cloud mapped with IRAM. Because continuum emission is rather strong towards W49, the flux of the CO lines may be (slightly) underestimated by our method of baseline removal. In order to account for this, we eye-estimated the continuum flux at 3 and 1.3 mm from the maps by Sievers et al. (1991). At 3 mm the flux ranges from 0.9 to 2.1 Jy/beam, which corresponds to a correction on the CO column density not larger than 20%.

In conclusion, when applying this factor, we obtain $N(C^{18}O) \leq 7 \times 10^{14} \text{ cm}^{-2}$ and $N(\text{CO}) \leq 3.5 \times 10^{17} \text{ cm}^{-2}$, using the standard value for the abundance ratio, $\text{CO}/C^{18}O = 500$. Finally, note that the highest column density in the mapped region is observed in a position, $(0'', 40'')$, at the border of the ISO-LWS beam, where a value $N(\text{CO}) = 7 \times 10^{17} \text{ cm}^{-2}$ is derived.

3.3. Location of the HD absorption

Figures 2 and 4 show that the position observed with ISO-LWS is not centered on the peak of the ^{13}CO and $C^{18}O$ emission at 63.5 km s^{-1} . We used the highest spatial resolution map available in the FIR at $53 \mu\text{m}$ (Harvey et al. 1977) obtained with the KAO ($FWHM = 25''$). We checked that the high resolution IRAS map (Ward-Thompson et al. 1992) at $60 \mu\text{m}$ is similar to the $53 \mu\text{m}$ one. Unfortunately, the W49 $100 \mu\text{m}$ IRAS data are saturated, preventing the construction of a high resolution map at this wavelength. Nevertheless, high resolution mapping of W49 in the submillimeter range ($450 \mu\text{m}$), performed at JCMT by Buckley & Ward-Thompson (1996), supports the idea that the continuum emission around $112 \mu\text{m}$ has a similar spatial distribution to that observed at $53 \mu\text{m}$. By superposing the $53 \mu\text{m}$ contours and the $C^{18}O$ (1–0) contours in the LWS beam, we estimate that about 50% of the FIR continuum flux comes through the molecular cloud and hence can be absorbed by it. This shows that the estimate of the HD column density derived in Sect. 3.1 is a lower limit while the estimate of the CO column density derived in Sect. 3.2 is an upper limit. We can therefore definitely argue that the values discussed in the next section are very conservative.

4. Discussion and conclusions

First, one can note that this result cannot be explained by a collection of translucent clouds along the line of sight, since HD and CO have similar variations with depth into the cloud (i.e., because of the lack of HD self-shielding, the $D \rightarrow HD$ transition occurs at about the same depth as the $C^+ \rightarrow CO$ conversion). Therefore, we assume that HD absorption and CO emission originate from the same cloud. There are at least $8 \times 10^{18} \text{ cm}^{-2}$ HD molecules in the cloud which absorb the $112 \mu\text{m}$ photons at 63.5 km s^{-1} and not more than $7 \times 10^{17} \text{ cm}^{-2}$ of CO molecules in the same cloud. The *minimum* $[HD]/[CO]$ ratio is therefore equal to 12. Assuming a standard CO abundance of 1×10^{-4} with respect to H_2 (van Dishoeck & Blake 1998) would give $[HD]/[H_2] > 1 \times 10^{-3}$ and therefore $D/H \geq 1 \times 10^{-3}$, i.e. *about two orders of magnitude larger than the average $[D]/[H]$ in the solar neighborhood!* (2×10^{-5} , Linsky et al. 1995; Linsky & Wood 1996; Sonneborn et al. 2000). The alternative to this extremely large $[D]/[H]$ ratio is to have an extremely small $[CO]/[H_2]$ ($\sim 1 \times 10^{-6}$) ratio. Either way, it is clear that the cloud absorbing the $112 \mu\text{m}$ photons is extreme and deserves further attention.

Since the primordial deuterium can only be destroyed (in the interiors of the stars), it is extremely unlikely that $[D]/[H] \geq 3.4 \times 10^{-5}$, the largest ever $[D]/[H]$ observed value (O'Meara et al. 2001). Although extreme, it is much more likely that the solution to this puzzle is a very low CO abundance in this cloud, among the lowest CO abundance ever measured in our Galaxy. It is possible that this cloud is very dense and cold and that depletion is particularly efficient there, maybe for the lack of an efficient mechanism to release back the molecules frozen onto the grain mantles. Previous cases of relatively low CO abundances in molecular clouds have been reported, which show that in some clouds the CO abundance (with respect to H_2) can be as low as 1×10^{-5} (Lis & Goldsmith 1989; Caux et al. 1999; Kramer et al. 1999; Vastel et al. 2000). In pre-stellar cores, "local" depletion of CO up to a factor 100 has been measured as well (e.g. Caselli et al. 1998), and also in some protostars large (~ 10) CO depletions have been observed (e.g. van Dishoeck et al. 1995; Lefloch et al. 1998).

Recent modeling of the L1544 pre-stellar core shows that indeed the CO abundance in the inner 2000 AU region can be lower than 1×10^{-6} (Caselli et al. 2002), a value similar to what we find. Of course, the cloud absorbing the $112 \mu\text{m}$ photons is much more massive than L1544. Assuming a kinematic distance of 6 kpc for the absorbing cloud, its mass (in one IRAM beam) is larger than $10^3 M_\odot$.

Further studies are needed to better understand the nature of this extreme cloud and to understand how unique it is in our Galaxy.

Acknowledgements. We thank E. F. van Dishoeck and C. M. Wright for planning these observations and for discussions on the data reduction and analysis. We also warmly thank the Director of IRAM, M. Grewing, for awarding Discretionary time, as well as C. Thum for an efficient organization of the observations and T. Gallego for doing the observations

themselves at the 30-m telescope. The CSO is funded by NSF contract AST 96-15025. The research of J. R. Pardo is funded by Spanish MCyT grant AYA 2000-1784.

References

- Abgrall, H., Roueff, E., & Viala, Y. 1982, *A&AS*, 50, 505
 Bertoldi, F., Timmermann, R., Rosenthal, D., et al. 1999, *A&A*, 346, 267
 Buckley, H. D., & Ward-Thompson, D. 1996, *MNRAS*, 281, 294
 Caselli, P., Walmsley, C. M., Terzieva, R., & Herbst, E. 1998, *ApJ*, 499, 234
 Caselli, P., Walmsley, C. M., Zucconi, A., et al. 2002, *ApJ*, in press
 Caux, E., Ceccarelli, C., Castets, A., et al. 1999, *A&A*, 347, L1
 Clegg, P. E., Ade, P. A. R., Armand, C., et al. 1996, *A&A*, 315, L38
 van Dishoeck, E. F., Blake, G. A., Jansen, D. J., & Groesbeck, T. D. 1995, *ApJ*, 447, 760
 van Dishoeck, E. F., & Blake, G. A. 1998, *ARA&A*, 36, 317
 Evenson, K. M., Jennings, D. A., Brown, J. M., et al. 1988, *ApJ*, 330, L135
 Ferlet, R., André, M., Hébrard, G., et al. 2000, *ApJ*, 538, L69
 Gry, C., Swinyard, B. M., Andrew, A., et al. 2001 (ESA Publication), SAI-99-077/Dc, version 1.2
 Gwinn, C. R., Moran, J. M., & Reid, M. J. 1992, *ApJ*, 393, 149
 Harvey, P. M., Campbell, M. F., & Hoffmann, W. F. 1977, *ApJ*, 211, 786
 Kessler, M. F., Steinz, J. A., Anderegg, M. E., et al. 1996, *A&A*, 315, L27
 Kramer, C., Alves, J., Lada, C. J., et al. 1999, *A&A*, 342, 257
 Lefloch, B., Castets, A., Cernicharo, J., et al. 1998, *A&A*, 334, 269
 Lis, D. C., & Goldsmith, P. F. 1989, *ApJ*, 337, 704
 Linsky, J. L., Diplas, A., Wood, B. E., et al. 1995, *ApJ*, 451, 335
 Linsky, J. L., & Wood, B. E. 1996, *ApJ*, 463, 254
 Moos, H. W., Cash, W. C., Cowie, L. L., et al. 2000, *ApJ*, 538, L1
 Nyman, L. A. 1983, *A&A*, 120, 307
 O'Meara, J. M., Tytler, D., Kirkman, D., et al. 2001, *ApJ*, 552, 718
 Polehampton, E. T., Baluteau, J.-P., Ceccarelli, C., et al. 2002, submitted to *A&A*
 Scoville, N. Z., & Solomon, P. M. 1973, *ApJ*, 180, 31
 Sievers, A. W., Mezger, P. G., Gordon, M. A., et al. 1991, *A&A*, 251, 231
 Sonneborn, G., Tripp, T. M., Ferlet, R., et al. 2000, *ApJ*, 545, 277
 Spitzer, L. 1978, *Physical Processes in the Interstellar Medium* (John Wiley & Sons editors), 52
 Swinyard, B. M., Burgdorf, M. J., Clegg, P. E., et al. 1998, *SPIE*, 3354, 888
 Vastel, C., Caux, E., Ceccarelli, C., et al. 2000, *A&A*, 357, 994
 Vidal-Madjar, A., Ferlet, R., & Lemoine, M. 1998, *SSR*, 84, 297
 Ward-Thompson, D., Berry, D. S., & Robson, E. I. 1992, *MNRAS*, 257, 180
 Wright, C. M., van Dishoeck, E. F., Cox, P., et al. 1999, *ApJ*, 515, L29